High-resolution photoemission spectroscopy study of the single-domain Si(110)-16×2 surface

N. D. Kim,[1] Y. K. Kim,[1,2] C.-Y. Park,[1,2,*] H. W. Yeom,[3] H. Koh,[4] E. Rotenberg,[4] and J. R. Ahn[1,†]
[1]*Department of Physics and Institute of Basic Science, Sungkyunkwan University, Suwon 440-746, Korea*
[2]*CNNC, Sungkyunkwan University, Suwon 440-746, Korea*
[3]*Center for Atomic Wires and Layers and Institute of Physics and Applied Physics, Yonsei University, Seoul 120-746, Korea*
[4]*Advanced Light Source, Lawrence Berkeley National Laboratory, Berkeley, California 94720, USA*
(Received 26 December 2006; published 12 March 2007)

We have investigated the valence band structure and Si 2*p* photoemission spectra of the single-domain Si(110)-16×2 surface with higher resolution than previous studies. We found that the highest occupied surface state, reported to be dispersive in the previous studies, is resolved into the two surface states with flat energy dispersions. This reveals that the two surface states are not produced by Si π-bonded chains, as suggested in the previous studies, but originate from the building blocks with spatially localized electronic structures such as a Si tetramer and a Si adatom. Si 2*p* line shapes show directly five surface components without any curve fitting. Various atomic structure models, especially the adatom-tetramer-interstitial model, of the Si(110)-16×2 surface are considered to figure out the atomistic origins of the surface components and states.

DOI: 10.1103/PhysRevB.75.125309 PACS number(s): 68.35.Rh, 73.20.−r, 79.60.−i

I. INTRODUCTION

The understanding of geometric and electronic structures of reconstructed low-index Si surfaces has been essential for characterizing various adsorbate-induced surface reconstructions and for widening their applications. Among reconstructed low-index Si surfaces, Si(100)-2×1, Si(111)-7×7, and Si(110)-16×2, only the Si(110)-16×2 surface is still not well understood.[1,2] Furthermore, recently the interests for the Si(110) surface have continued to grow because of its potential applications. First, complementary metal-oxide semiconductor transistors, based on Si(110) wafers, were found to have better hole mobility than ones based on Si(100) wafers.[3] Second, the anisotropic structure of the Si(110) surface has been used as a template to grow nanowires.[4] Third, Si nanowires with small diameters were reported to grow along the [110] direction, having a hexagonal cross section of the (110) face and bounded by {111} and {100} facets.[5,6]

Despite such growing interests, the atomic structure of the Si(110)-16×2 surface is not established mainly because it is as complex as the Si(111)-7×7 surface.[1,2] Morphological studies reported that up-and-down terraces alternating regularly on the surface play a major role to maintain the long-range 16×2 reconstruction.[2,7–9] In particular, the arrangement of "pairs of pentagons," observed by scanning tunneling microscopy (STM), has been considered as a cornerstone in constructing its atomic structure model.[10,11] In order to explain such observations, several atomic structure models have been suggested, based on building blocks such as π-bonded chains, adatoms, tetramers, regular steps, and missing rows: stretched-hexagon adatom,[12] tetramer-interstitial,[10] five-membered adcluster,[11] and adatom-tetramer-interstitial (ATI) models [see Fig. 1(c)].[1] Recently, Stekolnikov *et al.* proposed that the most stable structure for the long-range 16×2 reconstruction can be produced by combining the ATI configuration with the regular step arrangement.[2] This reveals tetramers to donate electrons to adjacent adatoms, which reproduces well the pentagonal arrays of spot shapes in the STM images.[2]

In comparison to morphological studies, high-resolution electronic information of the Si(100)-16×2 surface has been relatively rare in figuring out the long-range 16×2 reconstruction and testifying its atomic structure models.[1] Cricenti *et al.* first reported the Si 2*p* spectra[13] and energy bands[14] of the Si(110)-16×2 surface, which gives an overall electronic insight for the surface. However, the insufficient energy reso-

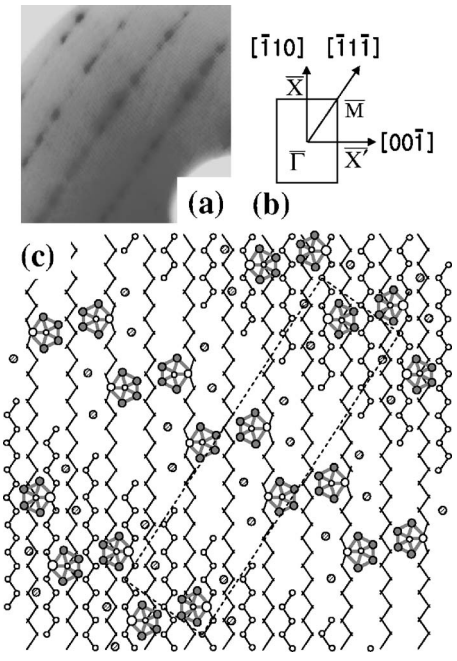

FIG. 1. (a) The LEED pattern of the clean Si(110)-16×2 surface and (b) 1×1 surface Brillouin zone. The schematic of the Stekolnikov *et al.* adatom-tetramer-interstitial model in (c) illustrates the sequence of pentagons and adatoms (the hatched circles) on up-and-down terraces. The pentagon consists of a tetramer atom (the filled circle), a first-layer atom (the open circle), and an interstitial atom located at its center (the small open circle). The dotted box indicates the unit cell of the 16×2 surface. Chains with (without) small open circles are the first-layer (second-layer) atoms.

lutions in the photoemission spectroscopy (PES) experiments prohibit observing accurate electronic information. Thus, the surface components of the Si $2p$ spectra were not decomposed directly from their line shapes, which provides uncertainty for the number of surface components and their binding energies.[13] Moreover, the insufficient energy resolution makes it difficult to define dispersions of energy bands, and a double-domain Si(110)-16×2 surface, used in the experiments, limits the determination of accurate energy bands along symmetric directions.[14]

In this paper, we measured extensively the high-resolution valence band structure and Si $2p$ photoemission spectra of the single-domain Si(110)-16×2 surface. The present valence band spectra reveal two surface states to locate at binding energies below 1 eV and to have flat energy dispersions along all symmetric directions. This suggests that the atomic structure of the Si(110)-16×2 surface should consist of building blocks with spatially localized electronic structures. Moreover, the surface components of the Si $2p$ photoemission spectra were directly resolved from their line shapes measured at various emission angles and photon energies. This makes it possible to determine obviously the number of surface components and their binding energies. Most of the photoemission spectral features are well explained by the Stekolnikov *et al.* ATI model with regular steps arrangement among various atomic structure models.

II. EXPERIMENT

The photoemission measurements were performed at two different locations. Si $2p$ core-level photoemission spectra were measured at a soft x-ray beamline (BL-8A1) connected to an undulator of the synchrotron radiation source at the Pohang Light Source (PAL) in Korea. The endstation is equipped with a high-resolution electron analyzer (SES-2002, Gamma Data, Sweden). The overall instrumental energy resolution, defined by photon beam and electron analyzer, is better than 40 meV and the acceptance angle of the analyzer is ±8°. The Si $2p$ core-level photoemission spectra were taken at 90 K in order to enhance the resolution by reducing the thermal broadening and were analyzed by a standard nonlinear-least-squares fitting procedure using Voigt functions. Angle-resolved photoemission spectra were measured with a photon energy ($h\nu$) of 90 eV and the energy-distribution curve mode, using an undulator synchrotron radiation at the beamline 7.0.1.2 of the Advanced Light Source (ALS) and a high-resolution electron energy analyzer (SES-100, Gamma Data, Sweden). The nominal energy and angular resolutions were better than 15 meV and 0.15°, respectively. The well-ordered Si(110) surface was prepared by repeated cycles of flashing at 1200 °C and subsequent annealing at 700 °C. This procedure produced a well-defined 16×2 LEED pattern, as shown in Fig. 1(a).[7]

III. RESULTS AND DISCUSSION

A. Angle-resolved photoemission spectroscopy

The valence band spectra of the clean Si(110)-16×2 surface were extensively measured. Representative valence band spectra along the three symmetry directions, $[00\bar{1}]$ ($\bar{\Gamma}$-$\bar{X}'$), $[\bar{1}1\bar{1}]$ ($\bar{\Gamma}$-$\bar{M}$), and $[\bar{1}10]$ ($\bar{\Gamma}$-$\bar{X}$), are shown in Figs. 2 and 3. No discernible photoemission intensity is observed from the Fermi energy to the binding energy E_b of 0.2 eV. This indicates that the clean Si(100)-16×2 surface is semiconducting, which is consistent with the Stekolnikov *et al.* theoretical calculations.[2] The valence band spectra show various different spectral features with large and small dispersions. In the valence band spectra along $\bar{\Gamma}$-$\bar{X}'$, four energy bands, S_1, S_2, U_1, and U_2, are found to be nearly flat with bandwidths below 0.2 eV, while other two energy bands, B_1 and B_2, are dispersive with bandwidths at least larger than 2 eV. The flat energy dispersion is one of characteristic features of surface bands, as observed on the Si(111)-7×7 surface,[15] and the S_1 and S_2 bands are located within the bulk-band gap. For these reasons, the S_1 and S_2 bands can be assigned as surface bands with E_b's of 0.4 and 0.9 eV, respectively. Other two dispersive bands, B_1 and B_2, are located within the projected bulk bands and are consistent with bulk bands observed in the previous studies.[16] We thus assign the B_1 and B_2 bands as bulk ones. The S_1 and S_2 surface bands were also noticed along other symmetric directions, $\bar{\Gamma}$-$\bar{M}$ and $\bar{\Gamma}$-$\bar{X}$, and were also found to be flat. The U_1 and U_2 bands, observed along the $\bar{\Gamma}$-$\bar{X}'$ and $\bar{\Gamma}$-$\bar{M}$ directions, and the U_3 band, observed along the $\bar{\Gamma}$-$\bar{X}$ direction have flat energy dispersions, but are located within the projected bulk bands. It is thus not obvious whether the U_1, U_2, and U_3 bands are

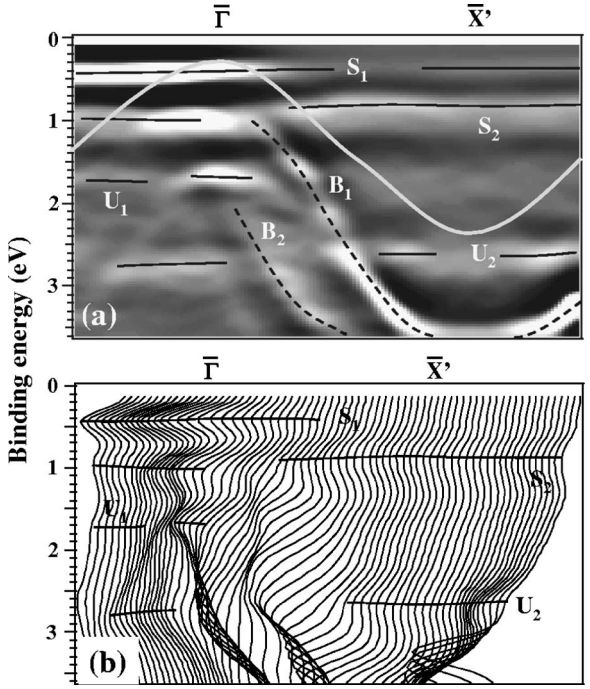

FIG. 2. The experimental band dispersion for the Si(110)-16×2 surface shown in (a) grayscale E_b−$k_{\|}$ diagram as well as (b) corresponding angle-resolved photoemission spectra taken along the $\bar{\Gamma}$-$\bar{X}'$ ($[00\bar{1}]$) direction using $h\nu$=90 eV. The edges of the bulk band projected onto the 1×1 surface Brillouin zone is drawn by the gray solid line. Two surface, two bulk, and two unknown states are denoted by S_1-S_2, B_1-B_2, and U_1-U_2, respectively.

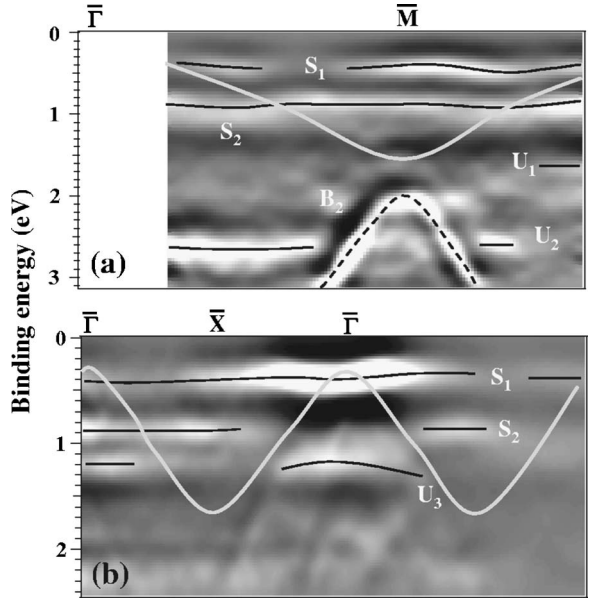

FIG. 3. The experimental band dispersion for the Si(110)-16×2 surface shown in grayscale $E_b-k_{\parallel}$ diagram along the (a) $\bar{\Gamma}$-$\bar{M}$ ([$\bar{1}1\bar{1}$]) and (b) $\bar{\Gamma}$-$\bar{X}$ ([$\bar{1}10$]) directions using $h\nu$=90 eV. The unknown state is denoted by U_3.

surface ones or not. In the previous study using a double-domain Si(110)-16×2 surface,[14] Cricenti *et al.* found that a surface band, located at E_b=0.6 eV, is dispersive along $\bar{\Gamma}$-$\bar{X}$ with a large bandwidth of 0.5 eV. However, the present extensive high-resolution study unveils that the surface band is not a single one and is rather composed of the two surface bands, *S*1 and *S*2, with small bandwidth below 0.2 eV.

The present finding is important because the dispersions of the surface bands are crucial in finding out the atomistic origins of the surface bands and in building up an atomic structure model. In order to speculate on atomistic origins of the surface bands, we resort to the atomic structure models of the Si(110)-16×2 surface. As introduced above, stretched-hexagon adatom,[12] tetramer-interstitial,[10] five-membered adcluster,[11] and ATI models[1] have been suggested, which are based on common building blocks such as π-bonded chains, adatoms, tetramers, regular steps, and missing rows. Recently, Stekolnikov *et al.* performed total-energy calculations with the large 16×2 unit cell using density functional theory. This suggested that the ATI model among the atomic structure models is the most stable structure in energetics and reproduces well the characteristic features of STM images, "pairs of pentagon" and alternative raised and lowered strips. The ATI model is based on the π-bonded chains buckled in opposite directions and one-half of the first-layer atoms removed. Adatoms and tetramers with interstitials are arranged on the buckled π-bonded chains and stabilizes the chains saturating their dangling bonds, as shown in Fig. 1(c).

Based on the dispersive surface band with the smallest E_b along $\bar{\Gamma}$-$\bar{X}$, Cricenti *et al.* suggested that the surface band is due to the π-bonded chains parallel to the [$\bar{1}10$] direction, as observed on the Si(111)-2×1 surface composed of π-bonded chains.[17–19] On the contrary, the present observation of the flat energy dispersions of the surface bands reveals the S_1 and S_2 bands not to originate from the π-bonded chain. The S_1 and S_2 bands could be rather due to building blocks with spatially localized electronic structures such as the tetramers, adatoms, and unsaturated π-bonded chains near step edges of the ATI model. The filled-state STM image taken at a bias voltage of −1.0 V exhibits only the tetramers and adatoms in the unit cell, which is reproduced by theoretical calculations based on the ATI model.[2,10] This leads to the conclusion that the S_1 and S_2 bands with E_b's below 1 eV are related to the tetramers and adatoms. In the ATI model, charge is transferred from the tetramers to the adatoms, so that the adatoms are expected to have a higher E_b than the tetramers. This supports that the S_1 and S_2 bands are produced by the tetramers and adatoms, respectively.

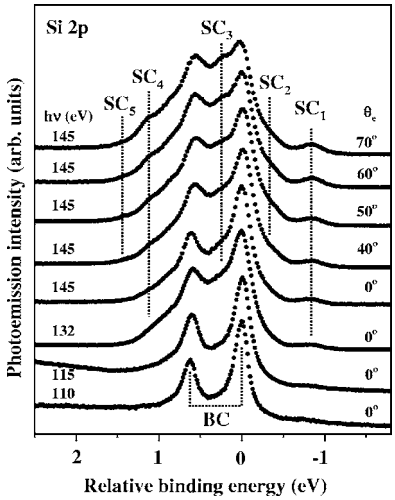

FIG. 4. Si 2*p* core-level spectra taken at 130 K with various $h\nu$'s and θ_e's. The surface and bulk components causing the spectral shape variation are indicated by dotted lines.

The surface bands could be understood further by the resemblance of the Si(110)-16×2 surface with the Si(111)-7×7 surface. Both surfaces are stabilized by long-range reconstructions and total energies are lowered by charge transfers between adatoms and rest atoms on the Si(111)-7×7 surface and between tetramers and adatoms on the Si(110)-16×2 surface. The E_b's and energy dispersions of the surface bands of the Si(111)-7×7 are also analogous to those of the Si(110)-16×2 surface.[15] Two surface bands on the Si(111)-7×7 surface, originating from adatoms and rest atoms, respectively, are flat with bandwidths below 0.2 eV and are located at E_b's of 0.15 and 0.9 eV, respectively. The charge transfer from the adatoms to the rest atoms on the Si(111)-7×7 surface lowers the energy level of the rest atom. This also supports the assignments of the S_1 and S_2 surface bands of the Si(110)-16×2 surface as due to the tetramers and adatoms, respectively, based on the charge transfer from the tetramers to the adatoms.

B. Si 2*p* core-level photoemission spectroscopy

Figure 4 shows the Si 2*p* spectra of the clean Si(110)-16×2 surface measured at various $h\nu$'s and emis-

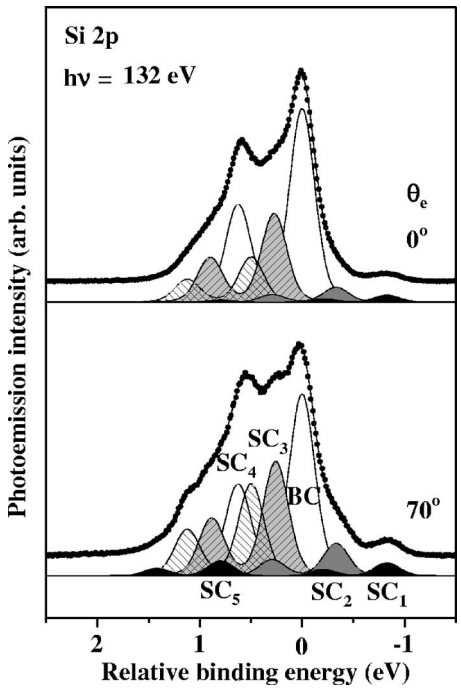

FIG. 5. Decomposition of the Si $2p$ core-level spectra taken at $h\nu$=132 eV and θ_e=0° and 70°. One bulk component, *BC*, and five different surface components, SC_1-SC_5, are introduced. SCLS's are given as −0.83, −0.33, 0.26, 0.50, and 0.70 eV for SC_1-SC_5, respectively.

sion angles (θ_e). The spectrum at the bottom of Fig. 4, measured at $h\nu$=110 eV and θ_e=0°, is the most bulk-sensitive one and is composed of nearly only the bulk component *BC*. With increasing $h\nu$ and θ_e, the spectra become more surface sensitive. At $h\nu$=132 eV, the Si $2p$ spectrum shows extra line shapes not overlapped with the *BC* component, which directly indicates the existence of surface components. A peak shape, assigned as the surface component SC_1, is noticed at a lower binding energy relative to that of the *BC* component [hereafter surface core-level shift (SCLS)]. Between the two spin-orbit-split *BC* components, the line shape is filled up at a surface sensitive $h\nu$, which is contributed by the surface component SC_3. Another change of the line shape is observed as a shoulder near a SCLS of 1 eV, which is assigned as due to the surface component SC_4. Besides, with increasing θ_e at the fixed $h\nu$=145 eV, two more surface components are noticed from their line shapes. A shoulder shape evolves between the *BC* and SC_1 components, which is assigned as due to the surface component SC_2. Another surface component SC_5 is observed at the tail of the line shape in the side of the positive SCLS.

The five surface components (SC_1-SC_5) and one bulk component (*BC*) are introduced in a schematic curve fitting analysis in order to reproduce the whole Si $2p$ line shapes. The fitting procedure proves that the six components reproduce consistently all Si $2p$ core-level spectra measured at various $h\nu$'s and θ_e's, where representative fitting results are shown in Fig. 5. Here, the Gaussian and Lorentzian widths are 0.26 and 0.06 eV, respectively. The line shape and curve fitting analysis find obviously that the Si $2p$ core-level spectrum of the Si(110)-16×2 surface is composed of five surface components: the SCLS's of the SC_1, SC_2, SC_3, SC_4, and SC_5 components are −0.83, −0.33, 0.26, 0.50, and 0.70 eV, respectively. In the previous studies,[13] the number of surface components were determined only from the curve fitting analysis because of a lack of an energy resolution and their SCLS's thus were not accurate. In comparison, the present Si $2p$ line shapes resolve conclusively the surface components and make it possible to determine accurately their SCLS's.

To connect the building blocks of the atomic structure model of the Si(110)-16×2 surface with the surface components, we need to refer the previous assignments of the Si $2p$ core-level spectra of Si surfaces with well-established atomic structure models. The building blocks of the ATI model with distinctively different bonding characters from the bulk sp^3 bond are tetramers, interstitials, adatoms, and unsaturated π-bonded chains at step edges. We first consider the SC_1 and SC_2 components with negative SCLS's of −0.83 and −0.33 eV, respectively. The rest atom on the Si(111)-7×7 surface and the π-bonded chains on the Si(111)-2×1 surface are known to produce surface components with negative SCLS's of −0.70 and −0.44 eV, respectively. In the ATI model, Stekolnikov *et al.* show that charges are transferred from the tetramers to the adatoms. This indicates that the adatom with charge gain on the ATI model is similar to the rest atom on the Si(111)-7×7 surface. Additionally, a part of the underlying π-bonded chains at step edges are not saturated by tetramers or adatoms. The adatoms and unsaturated π-bonded chains thus could produce the SC_1 and SC_2 components. Second, we take the surface components, SC_3, SC_4, and SC_5, with positive SCLS's into account. Among five surface components, the SC_3 component is the least surface sensitive, has the largest intensity, and is located near the *BC* component, as shown in Fig. 5. This implies that the second-layer Si atoms could produce the SC_3 component, as observed on the Si(100)-2×1 and Si(111)-7×7 surfaces.[15,20] The intensity of the SC_4 component is remarkably larger than other surface components except the SC_3 component. Thus, the underlying π-bonded chains, occupying the most surface atoms in the unit cell, could be the origin of the SC_4 component.[15,20] The tetramers could also be one of the origins of the surface component with positive SCLS's because the tetramers are positively charged due to the charge transfer from the tetramers to the adatoms. A part of the tetramer is expected to be involved in the charge transfer so that the actual number of Si atoms in the unit cell is below 16, where the number of underlying π-bonded chains in the unit cell is 52. When considering the intensity of the SC_5 component relative to those of other surface components, it is likely that the SC_5 component comes from a part of the tetramer.

IV. CONCLUSION

The single-domain Si(110)-16×2 surface has been studied by high-resolution angle-resolved and Si $2p$ core-level photoemission spectroscopy. In the valence band spectra, we identified two distinct surface states with E_b's of 0.4 and 0.9 eV, respectively. The flat energy dispersions of the two

surface states imply that the Si(110)-16×2 structure is composed of building blocks with spatially localized electronic structures such as a tetramer and an adatom. We suggests that the two surface states with E_b's of 0.4 and 0.9 eV originate from the tetramer with the interstitial and the adatom, respectively, based on the adatom-tetramer-interstitial model. Additionally, the high resolution Si $2p$ spectra allow to resolve five surface components with SCLS's of −0.83, −0.33, 0.26, 0.50, and 0.70 eV, respectively. Based on the ATI model, the SC_1 and SC_2 components with negative SCLS's may be due to the adatom and the unsaturated π-bonded chain at the step edge, while the SC_4 and SC_5 components with positive SCLS's may come from the underlying π-bonded chain and tetramer, respectively.

ACKNOWLEDGMENTS

This work was supported by the Korea Research Foundation Grant funded by the Korean Government (MOEHRD) (Grant No. KRF-2006-312-C00120) and Korea Science Foundation through the SRC program (Center for Nanotubes and Nanostructured Composites) of MOST/KOSEF. One of the authors (J.R.A.) is also supported by the Korea Research Foundation Grant funded by the Korean Government (MOEHRD) (Grant No. KRF-2005-005-J11903). One of the authors (H.W.Y.) is supported by MOST through Center for Atomic Wires and Layers of the CRi program. The Advanced Light Source is operated under DOE contract at Lawrence Berkeley National Laboratory.

*Author to whom all correspondence should be addressed. Electronic address: cypark@skku.edu

†Electronic address: jrahn@skku.edu

[1] A. A. Stekolnikov, J. Furthmüller, and F. Bechstedt, Phys. Rev. B **70**, 045305 (2004).

[2] A. A. Stekolnikov, J. Furthmüller, and F. Bechstedt, Phys. Rev. Lett. **93**, 136104 (2004).

[3] K. Arima, J. Katoh, S. Horie, K. Endo, T. Ono, S. Sugawa, H. Akahori, A. Teramoto, and T. Ohmi, J. Appl. Phys. **98**, 103525 (2005).

[4] S. Liang, R. Islam, D. J. Smith, P. A. Bennett, J. R. O'Brien, and B. Taylor, Appl. Phys. Lett. **88**, 113111 (2006).

[5] D. D. D. Ma, C. S. Lee, F. C. K. Au, S. Y. Tong, and S. T. Lee, Science **299**, 1874 (2003).

[6] T. L. Chan, C. V. Ciobanu, F. C. Chuang, N. Lu, C. Z. Wang, and K. M. Ho, Nano Lett. **6**, 277 (2006).

[7] H. Ampo, S. Miura, K. Kato, Y. Ohkawa, and A. Tamura, Phys. Rev. B **34**, 2329 (1986).

[8] A. J. Hoeven, D. Dijkkamp, E. J. van Loenen, and P. J. G. M. van Hooft, Surf. Sci. **211-212**, 165 (1989).

[9] Y. Yamamoto, Phys. Rev. B **50**, 8534 (1994).

[10] T. An, M. Yoshimura, I. Ono, and K. Ueda, Phys. Rev. B **61**, 3006 (2000).

[11] T. Ichikawa, Surf. Sci. **544**, 58 (2003).

[12] W. E. Packard and J. D. Dow, Phys. Rev. B **55**, 15643 (1997).

[13] A. Cricenti, G. Le Lay, V. Yu Aristov, B. Nesterenko, N. Safta, J. P. Lacharme, C. A. Sebenne, A. Taleb-Ibrahimi, and G. Indlekofer, J. Electron Spectrosc. Relat. Phenom. **76**, 613 (1995).

[14] A. Cricenti, B. Nesterenko, P. Perfetti, G. LeLay, and C. Sebenne, J. Vac. Sci. Technol. A **14**, 2448 (1996).

[15] R. I. G. Uhrberg, T. Kaurila, and Y.-C. Chao, Phys. Rev. B **58**, R1730 (1998).

[16] Y. K. Kim, J. R. Ahn, E. S. Cho, K.-S. An, H. W. Yeom, H. Koh, E. Rotenberg, and C. Y. Park, Surf. Sci. **596**, L325 (2005).

[17] K. C. Pandey, Phys. Rev. Lett. **47**, 1913 (1981).

[18] P. Mårtensson, G. V. Hansson, and P. Chiaradia, Phys. Rev. B **31**, 2581 (1985).

[19] R. I. G. Uhrberg, G. V. Hansson, J. M. Nicholls, and S. A. Flodström, Phys. Rev. Lett. **48**, 1032 (1982).

[20] E. Landemark, C. J. Karlsson, Y.-C. Chao, and R. I. G. Uhrberg, Phys. Rev. Lett. **69**, 1588 (1992).